

AUTOMATIC DETERMINATION OF OPTIMAL SURGICAL  
DRILLING TRAJECTORIES FOR COCHLEAR  
IMPLANT SURGERY

By

Jack H. Noble

Thesis

Submitted to the Faculty of the Graduate School of  
Vanderbilt University in partial fulfillment  
of the requirements for the degree of

MASTER OF SCIENCE

in

Electrical Engineering

December, 2008

Nashville, Tennessee

Approved:

Date:

J. Michael Fitzpatrick

December 5 2008

Benoit Dawant

December 5 2008

## **ACKNOWLEDGEMENTS**

I would like to thank my advisors, Drs. Benoit Dawant and J. Michael Fitzpatrick for their invaluable guidance throughout my research. I would also like to thank Drs. Omid Majdani and Robert Labadie for their help validating the results of this research. Finally, I am grateful to the NIH for their financial support.

# TABLE OF CONTENTS

	Page
ACKNOWLEDGEMENTS .....	ii
LIST OF FIGURES .....	iv
LIST OF TABLES .....	v
Chapter	
I. INTRODUCTION .....	1
II. CLINICAL RELEVANCE .....	3
III. PROBLEM FORMULATION .....	8
IV. METHODS .....	14
Introduction.....	14
Detecting surface contact.....	14
Detecting effectiveness .....	18
Probability of success calculations .....	20
Drilling trajectory optimization .....	22
V. EXPERIMENTAL RESULTS.....	24
VI. DISCUSSIONS AND CONCLUSIONS .....	32
REFERENCES .....	33

## LIST OF FIGURES

	Page
1. Anatomy of the ear.....	3
2. Intra-operative drill guide .....	6
3. Example of effective electrode insertion .....	9
4. 3-D rendering of ear structures .....	10
5. Example drilling trajectory in a CT image .....	11
6. Flow chart of the optimization routine.....	13
7. Example of distance map minimizers .....	16
8. Illustration of an effective surgical trajectory .....	19
9. 3-D rendering of optimized trajectories .....	28

## LIST OF TABLES

	Page
1. Probabilities of effectives and safety for experimental trajectories.....	25

# CHAPTER I

## INTRODUCTION

In recent years, on-going research has demonstrated the benefits of minimally invasive surgical approaches. These approaches typically attempt to inflict as little damage as possible to the patient while achieving the goal of the procedure. One particular sub-genre of minimally invasive procedures is stereotactic surgery, which has become a popular approach for neurosurgery and radiosurgery procedures [1]. With this type of procedure, some external markers are affixed to the patient. The position of anatomical targets with respect to the markers can be determined prior to surgery using an imaging modality. In the operating room, the position of these targets can be determined by tracking the external markers. A mechanical system is then used to constrain the motion of surgical devices with respect to those markers to appropriately target specified anatomy. In the case of highly constrained mechanical fixtures, physicians can accurately target internal anatomical structures without the need to directly see internal structures. Thus, this approach typically allows physicians to inflict a minimal amount of damage, since it is not necessary to excise tissue for the purpose of visually locating anatomical targets.

Recently, a minimally invasive stereotactic approach to cochlear implant surgery has been proposed, percutaneous cochlear implantation (PCI). Cochlear implantation is a surgical procedure in which an electrode array is permanently implanted in the cochlea to

stimulate the auditory nerve and allow deaf people to hear. Traditional techniques require wide excavation of the temporal bone to ensure that the surgeon does not damage sensitive structures. Percutaneous cochlear implantation requires drilling only a single hole on a straight trajectory from skull surface to the cochlea and allows the trajectory to be chosen pre-operatively in a CT. A major challenge with this approach is to determine, in the CT, a safe and effective drilling trajectory, i.e., a trajectory that with high probability avoids specific vital structures—the facial nerve, ossicles, external auditory canal, and chorda tympani—and effectively reaches the cochlea. These features lie within a few millimeters, the drill is one millimeter in diameter, and drill positioning errors are approximately a half a millimeter root-mean square. Thus, trajectory selection is both difficult and critical to the success of the surgery. An atlas-based method for automatic trajectory selection was recently presented but produces sub-optimal results. In this thesis, a method is presented for optimizing such trajectories with an approach designed to maximize safety under conditions of drill positioning error. Results are compared with trajectories chosen manually by an experienced surgeon. In tests on thirteen ears, the technique is shown to find approximately twice as many acceptable trajectories as those found manually.

## CHAPTER II

### CLINICAL RELEVANCE

Cochlear Implantation is a surgical procedure performed on individuals who experience profound to severe sensorineural hearing loss, i.e., individuals who are deaf. In normal ears, sound waves propagate through the external ear to the ear drum. Vibrations are amplified by the malleus, incus, and stapes before causing a fluid wave to travel in the inner ear, the cochlea (Figure 1).

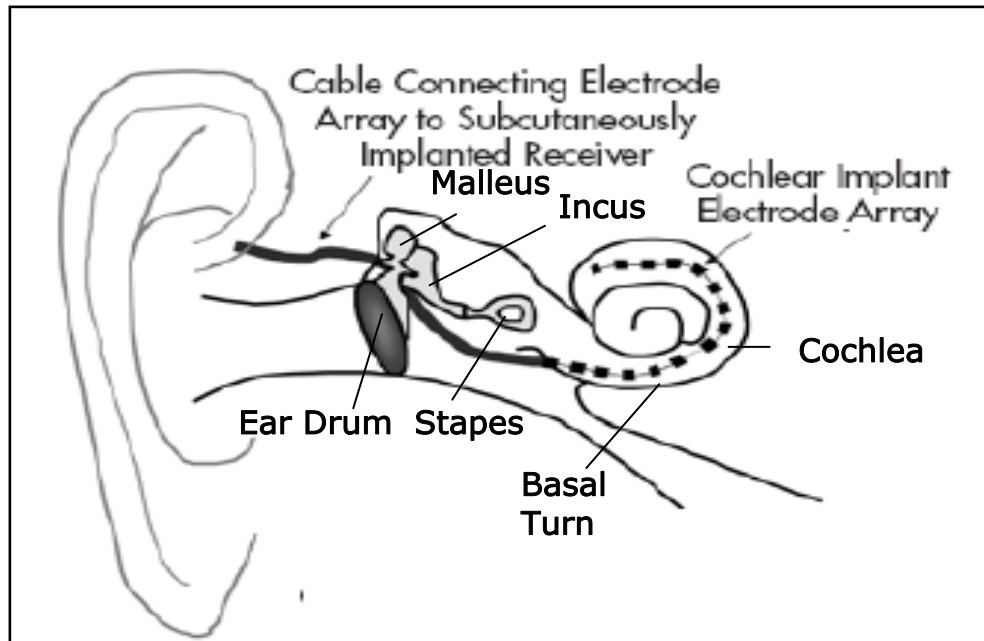


**Figure 1.** Anatomy of the ear. An electrode array is threaded through the basal turn into the cochlea.



This fluid wave travels over many tiny hair cells. The bending of these hair cells begins a complex molecular cascade that results in stimulation of the auditory nerve. The auditory nerve innervates an area of the brain which allows one to hear. The natural ability to hear can be hindered by damage to any of these structures. Cases involving less severe hearing loss are normally treated using hearing aids, which amplify the sound waves that impinge on the ear drum. When damage becomes severe, cochlear implants (CI's) are the preferred treatment. More than 80,000 implants have been placed worldwide, including 60,000 in the United States. Projections indicate that over 750,000 Americans with severe hearing loss may benefit from an implant [2].

In CI surgery, an electrode array is permanently implanted into the cochlea by threading the array through the basal turn (Figure 1). The array is connected to a receiver mounted securely under the skin behind the patient's ear. When activated, the external processor senses sound, decomposes it (usually involving Fourier analysis), and digitally reconstructs it before sending the signal through the skin to the internal receiver which then activates the appropriate intracochlear electrodes causing stimulation of the auditory nerve and hearing. Traditional approaches require wide excavation of the mastoid region of the temporal bone to visually locate and ensure the safety of sensitive structures. PCI bypasses this task by using a stereotactic frame to drill a single hole on a straight, mechanically constrained, path from the skull surface to the cochlea [3],[4],[5].

Several key advantages make PCI preferable over traditional methods. PCI would be a far less invasive surgery since a single hole is drilled to the cochlea rather than full

excavation of the mastoid region. Excavation is the most time consuming portion of the surgery since great care is needed to expose and avoid sensitive structures. By averting excavation, surgery time can be reduced from the current 2 to 3 hours down to as short as 30 minutes. PCI would standardize and simplify the surgical technique, which could allow less experienced surgeons to perform the surgery. Currently, patients must wait 1-3 weeks for implant activation as swelling from the open-field surgery is resolved. With a percutaneous approach, swelling no longer becomes an issue and activation can occur on the same day as surgery.

PCI is accomplished by performing preoperative planning using CT imagery to create an appropriate drill guide. Prior to surgery, anchors are affixed to the patient's skull by creating three small skin incisions and screwing self-tapping anchors into the bone. A CT image of the patient is acquired, and the image is used by the physician to pick a safe direct drilling trajectory from the skin surface to the cochlea. With the path and image information about anchor location, a drill guide unique to the patient is rapid prototyped. In surgery, the drill guide is attached to the bone implanted anchors on the patient's skull. The drill is attached to the guide, which governs the path of the drill all the way to the cochlea (Figure 2). This method of preoperative planning for drill guide construction was successful for Deep Brain Stimulator (DBS) procedures [6].

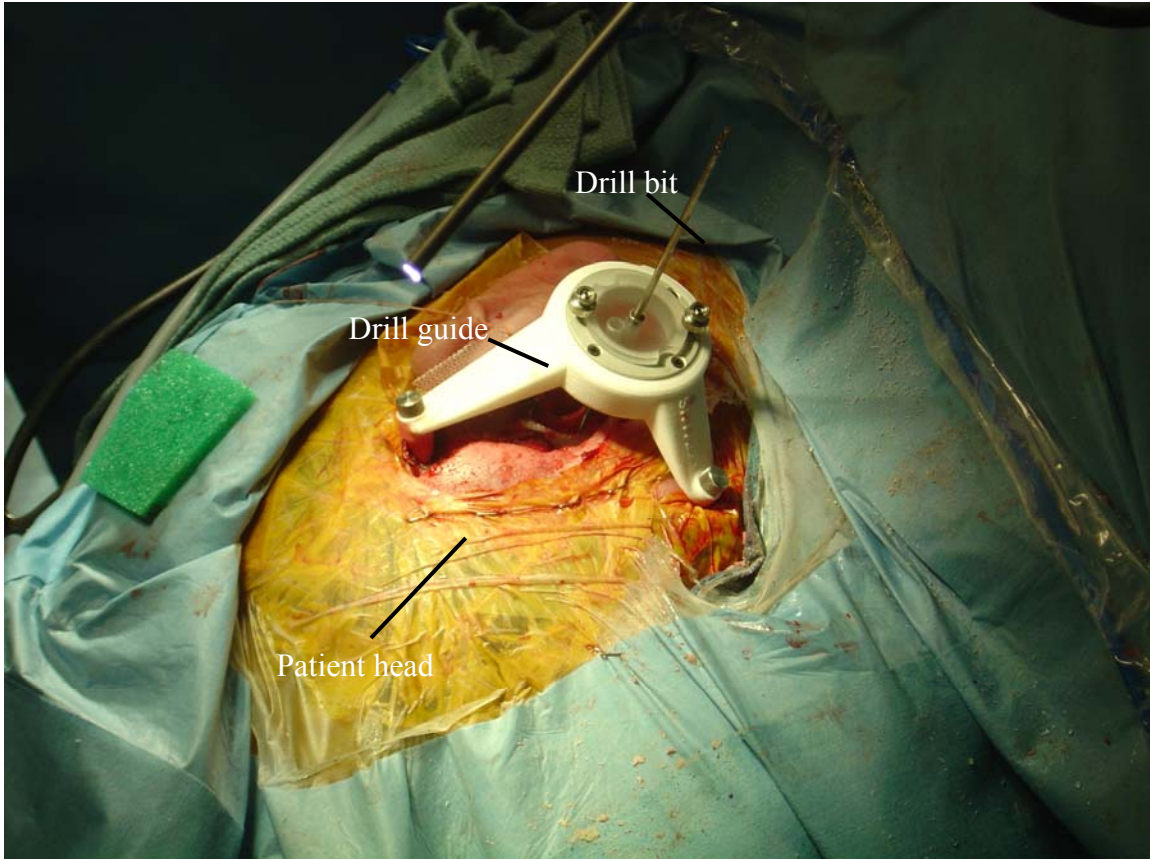


**Figure 2.** Picture taken during clinical testing of percutaneous CI method. The image shows a drill guide fixed to anchors implanted in a human skull.

Currently, the major problems with the proposed method of PCI are the various sources of error. Recent studies suggest that there is a root-mean-square (RMS) positioning error in the drill guide system of 0.44 mm at the specified target point [7]. A value of 0.44 mm RMS would be a safe estimation of the total error if it the physician were certain to choose the appropriate path in the preoperative CT. Choosing a path to avoid three-dimensional structures by examining a volume of two-dimensional images has proved to be quite difficult, even for experienced physicians. While finding a line segment to the cochlea that avoids sensitive structures is not so difficult, manually

choosing a safe line segment that accounts for the 1.0 mm diameter of the surgical drill burr as well as the 0.44 mm RMS error in the drill guide system is highly difficult, if not impossible, to do manually. These tasks can, however, be accomplished using automated algorithms.

## CHAPTER III

### PROBLEM FORMULATION

PCI can become a preferred solution only if the surgical method proves to be at least as effective and as safe as traditional methods. An effective CI drilling procedure can be simply defined as a procedure in which effective access to the cochlea is achieved. In optimal procedures, the CI electrode array can be threaded gently into the scala tympani, an internal cavity of the cochlea, at a tangential angle, through the round window overhang of the cochlea. Thus, an effective drilling trajectory is one that reaches the round window at a position and orientation that are conducive to easy and gentle electrode insertion into the scala tympani. An example of a successfully inserted electrode is shown in Figure 3.

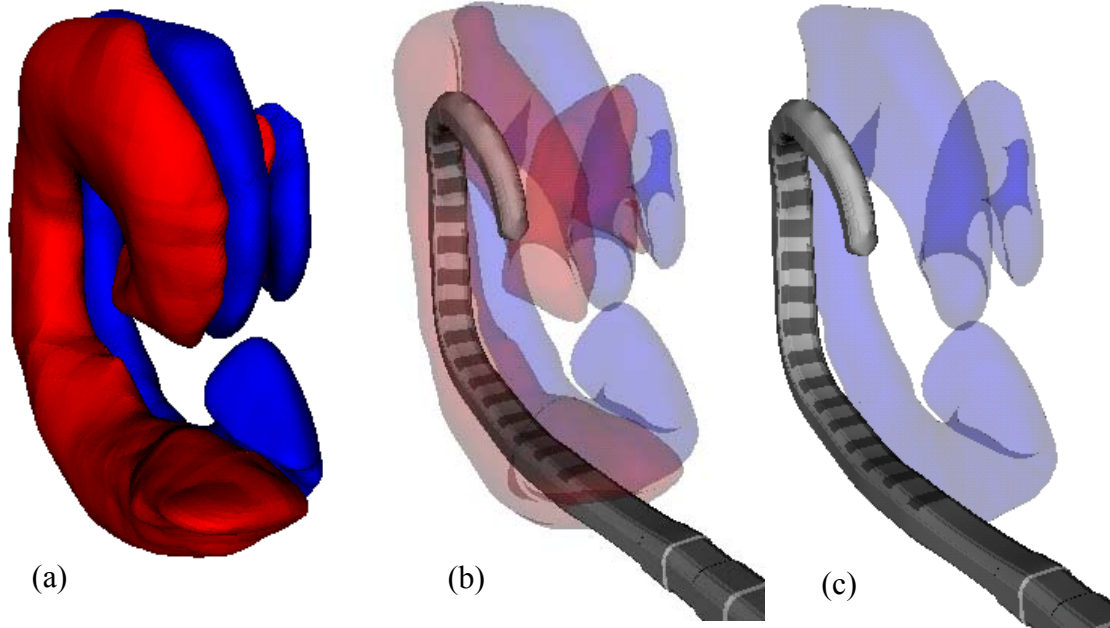


**Figure 3.** Example of an effective electrode insertion. Displayed are Scala Tympani (red) and Scala Vestibuli (blue) of an implanted patient. These surfaces are displayed transparently in (b) to show the electrode array inserted in the scala tympani. In (c), the scala tympani is removed to show that the array is completely in the scala tympani and not in the scala vestibuli.

Recent studies have shown that using traditional procedures, the current industry standard electrode arrays are properly inserted into the scala tympani at a success rate of approximately 73% [8].

A safe CI drilling procedure can be defined as a procedure in which sensitive anatomical structures encountered along the path to the cochlea are avoided. Thus, a safe drilling trajectory is a trajectory that is placed such that a surgical drill following the trajectory would not contact a sensitive structure before entering the cochlea. These structures include the facial nerve, the external auditory canal, the chorda tympani, and the ossicles. The facial nerve is a highly sensitive structure that controls all movement of

the ipsilateral face. If damaged, the patient may experience temporary or permanent facial paralysis. Violation of the external auditory canal can lead to a breach in sterility and open a potential avenue for future infection with possible implant extrusion. Injury to the chorda can result in temporary or permanent loss in the ability to taste. Chorda injury is undesirable, but may occur in as many as 20% of all CI surgeries and therefore is not considered catastrophic. Injury to the ossicles can result in damage to residual hearing, and therefore is also not currently considered catastrophic since implanted patients are already deaf. However, in the future, implants will most likely involve individuals with residual hearing where violation of the ossicles would be discouraged. Thus the ossicles are included as vital, adjacent structures. Figure 4 shows a 3D rendering of these structures.

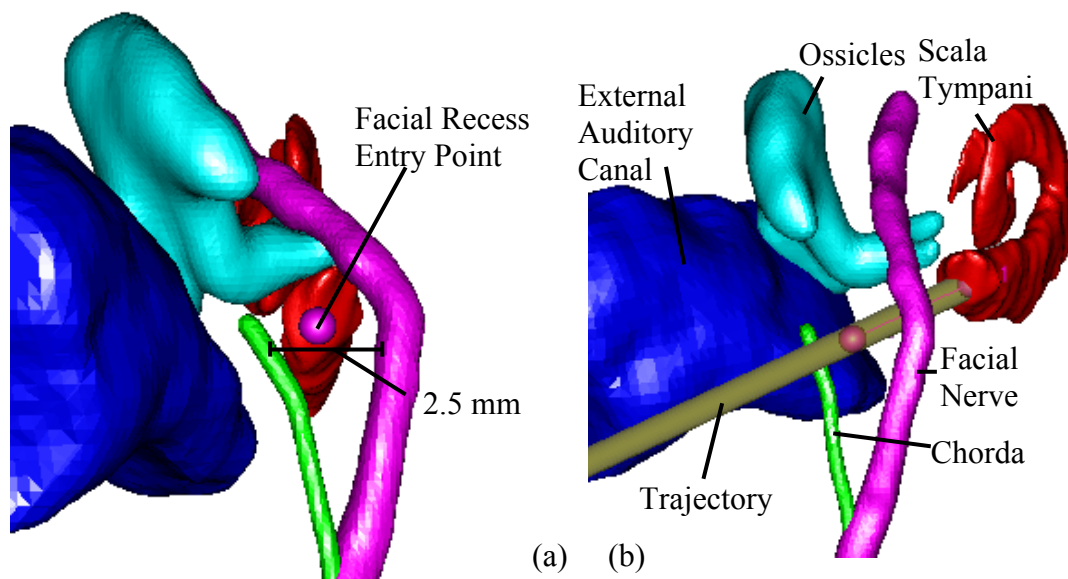


**Figure 4.** 3D rendering of the structures of the left ear. (a). Left-right, Posterior-Anterior view along the preferred drilling trajectory. The round window target point is located at the scala tympani surface. (b). Posterior-Anterior view. Included are the facial nerve, scala tympani, chorda, ossicles, and external auditory canal.

A CI drilling trajectory can be completely defined by a target point (at the scala tympani via the round window) and an entry point (at the surface of the skull). However, since vital anatomy occurs approximately 2 cm from the surface of the skull, the skull surface entry point is actually constrained by a deeper entry region, i.e., it does not matter where the lateral skull is entered as long as this deeper region's boundaries are not transgressed (see Figure 5).

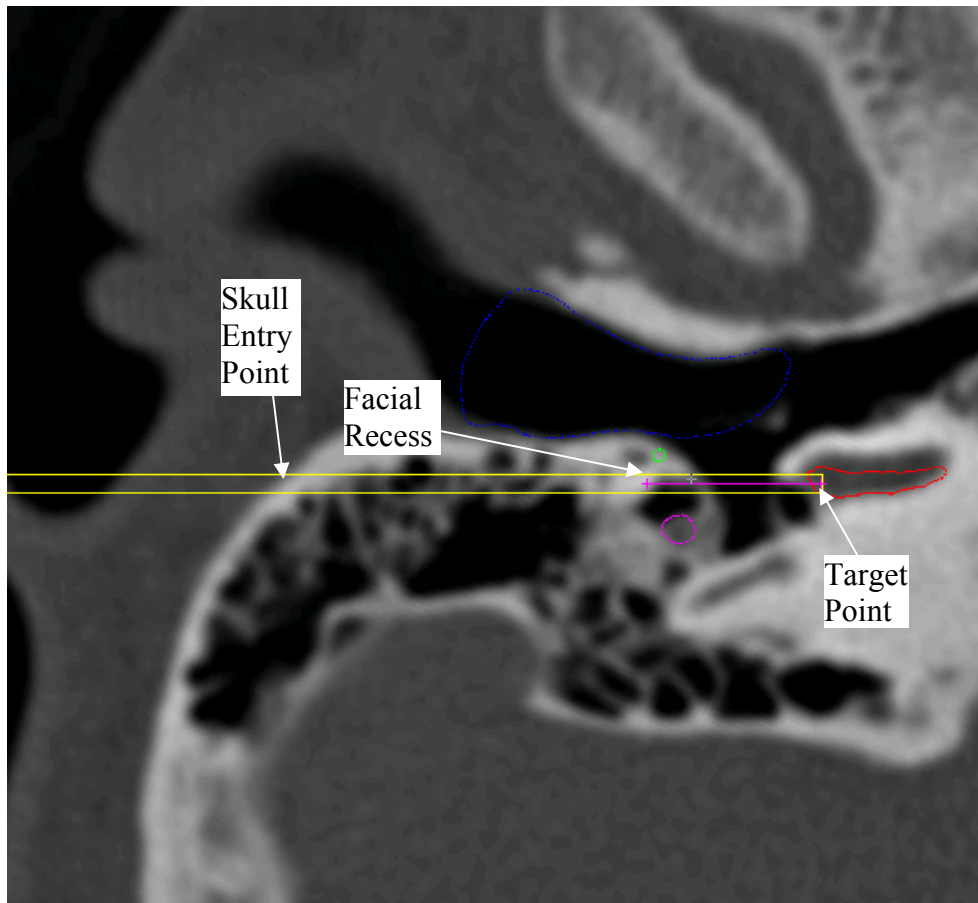


**Figure 5.** Target and entry points along surgical trajectory.



This region is termed the “facial recess” and is bounded by the facial nerve, the chorda tympani, and the body of one of the ossicles, the incus. In extreme cases, the chorda must be sacrificed to ensure the safety of the facial nerve. When this occurs, the entry region is no longer bounded by the chorda, but by the external auditory canal. When looking through the facial recess to the cochlea along the preferred drilling trajectory, it can be seen that the structures we wish to avoid create a window approximately 1.0-3.5mm in diameter through which a safe path to the cochlea can be planned (see Figure 4).

Recently, an atlas-based approach to automatically determine CI drilling trajectories has been proposed [9]. This method uses image registration techniques to map a specified target and entry point chosen manually in an atlas image onto any patient image, thus defining a drilling trajectory for the patient. Results that are later summarized in this manuscript will show that that this technique produces results that are reasonable but do not adequately guarantee safe and effective trajectories.

This thesis presents an approach to automatically find a safe and effective drilling trajectory by optimizing a reasonably placed trajectory, such as one extracted using the atlas-based technique, while accounting for error in the positioning of the surgical drill. To facilitate the approach, methods were developed to (1) detect whether a drill burr following an arbitrary drilling trajectory subject to zero error is safe, (2) detect whether a trajectory subject to zero error is effective, (3) compute the probability that a trajectory subject to non-zero error is safe and effective, and (4) automatically find a

probabilistically safe and effective drilling trajectory for access to the cochlea.

The general approach is illustrated in Figure 6. For any particular trajectory, probabilities that the trajectory is effective and that it will not damage each individual structure are estimated using Monte Carlo simulations, i.e., by iteratively perturbing the trajectory with error of the expected distribution and calculating the fraction of iterations for which the displaced trajectories are effective and safe with respect to each sensitive structure. Using a cost function, these probabilities are combined into a single number representing the “cost” for the trajectory. A probabilistically safe and effective drilling trajectory can then be found by using a minimization technique to optimize a roughly placed trajectory with respect to the cost function. The rest of this thesis details the methods.

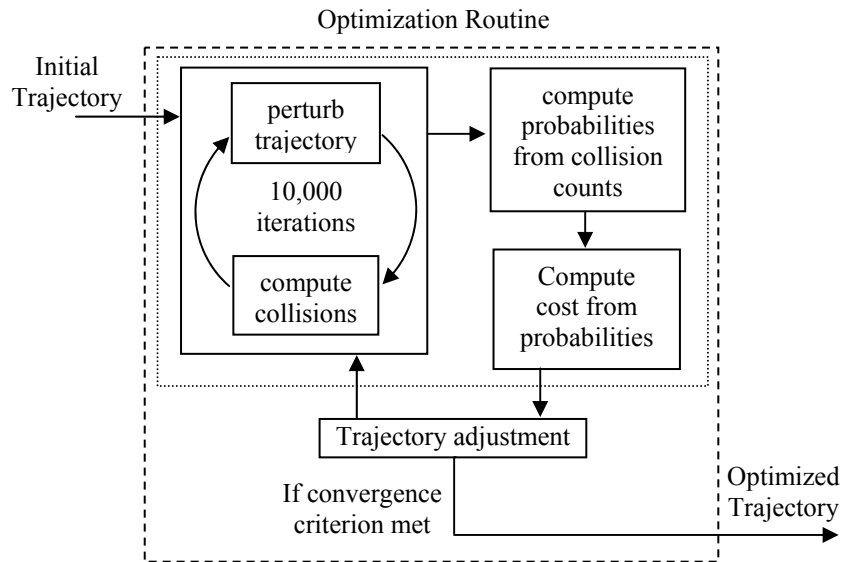


**Figure 6.** Approach for computing an optimally safe and effective surgical drilling trajectory.

## CHAPTER IV

### METHODS

#### Introduction

The proposed method to automatically plan a probabilistically safe and effective drilling trajectory requires some prior information. It is necessary to know the distribution of error along the trajectory, to know the radius of the surgical drill burr, and to have all sensitive structures localized and represented as signed distance maps aligned with the patient CT. A distance map can be extracted from a binary mask or a point set using, for instance, fast marching methods [10].

#### Detecting surface contact

In order to determine whether a given trajectory will cause the drill burr to contact a structure, we first need to be able to calculate the closest distance between the planned trajectory and the surface of the structure. Suppose there is a drill path line  $L$  which passes through entry point  $p_e$  and target point  $p_t$ . Any arbitrary point  $m$  on the line  $L$  can be represented as

$$\begin{aligned} m &= p_e + av, \\ v &= \frac{p_t - p_e}{\|p_t - p_e\|}, \end{aligned} \tag{1}$$

where  $a$  is some scalar. Suppose now that we have a surface  $S$  represented by distance map  $D_S$ . The value of a distance map at any given grid location (at any pixel or voxel) is the distance to the closest point on the zero-level set surface. The distance  $d$  between  $L$  and  $S$  can be calculated by

$$d = \text{dist}(S, L) = \min_a D_S(m(a)), \quad (2)$$

where evaluation of  $D_S$  is performed using trilinear interpolation of the grid values.

It is possible to estimate  $d$  by evaluating  $D_S$  along  $L$  at discrete intervals, e.g., by evaluating  $D_S$  at every one tenth of a voxel along  $L$  and choosing the minimum of all such evaluations. However, a much more precise and efficient method for computing  $d$  is to minimize the trilinear interpolant of  $D_S$  along  $L$  over each 8-voxel neighborhood through which  $L$  passes. A 2D version of the method is illustrated schematically in Figure 7.

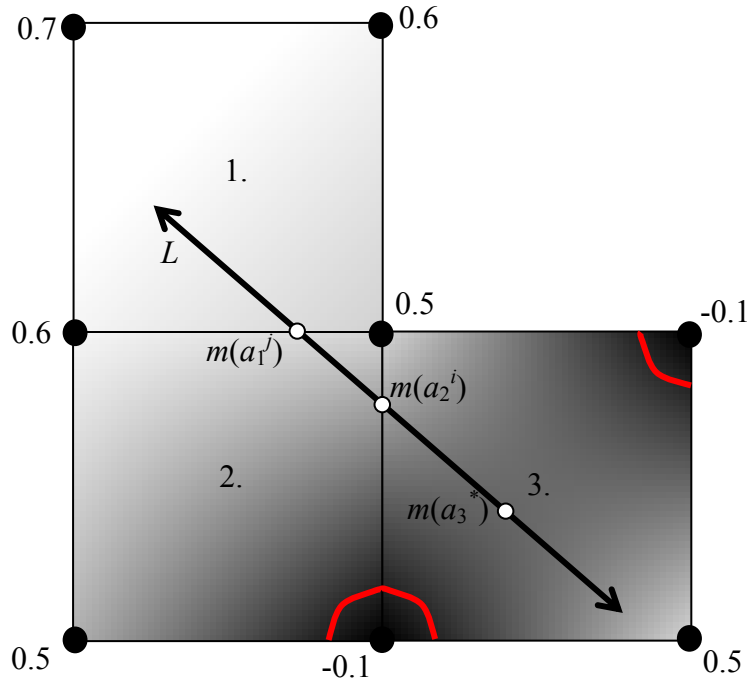


**Figure 7:** 2D example of the minimizer of a linear interpolant function along a line. The nodes denote pixel positions in the distance map, each with an assigned distance value. The gray level intensities illustrate the relative interpolated distance values between the known pixel values. The red contours indicate the position of the surface implied by the distance values. The minimizers along  $L$  of the interpolation function for three 4-pixel neighborhoods through which  $L$  passes (labeled 1, 2, and 3) are displayed, labeled as  $a_1$ ,  $a_2$ , and  $a_3$ .

In 2D, we again wish to find the minimum distance between a line  $L$  and a 2D surface represented by a 2D distance map  $D_S$ . This can be computed by determining the minimum distance map value along the continuous line  $L$ . Portions of  $L$  will no doubt pass between the distance map discrete-grid values; however, distances between grid values can be estimated using bilinear interpolation. Each square region on the grid bounded by a set of four pixel centers will be referred to as a neighborhood. Let us first

examine computation of the minimum distance in a single neighborhood along  $L$ ,  $d_N$ . The bilinear function used for interpolation within the neighborhood is defined by the four cornering pixel coordinates and their distance values. The pixels representing the corners of a neighborhood can be represented with the coordinates  $(x_i, y_j)$ ,  $(x_i, y_j+1)$ ,  $(x_i+1, y_j)$ ,  $(x_i+1, y_j+1)$ , and let the distance map values at each point be labeled  $g_{1-4}$ . Assume, for the sake of simplicity, and without loss of generality, that the coordinate system has been translated as a preprocessing step such that  $x_i = y_j = 0$ . Then, the bilinear function  $q(x, y)$  which defines distance values within the neighborhood can be written as

$$\begin{aligned}
q(x, y) &= Q_1 + Q_2x + Q_3y + Q_4xy, \\
Q_1 &= g_1 \\
Q_2 &= -g_1 + g_2 - g_3 + g_4 \\
Q_3 &= -g_1 - g_2 + g_3 + g_4 \\
Q_4 &= g_1 - g_2 - g_3 + g_4
\end{aligned} \tag{3}$$

Assume any point along  $L$  is represented as in Eq. (1), and the  $x$  and  $y$  components of  $p_e$  and  $v$  are represented by  $x_e, y_e, x_v$ , and  $y_v$ . Then the function  $q(x, y)$  evaluated at any point along  $L$  is a 1D quadratic function  $w(a)$  and can be represented as

$$\begin{aligned}
w(a) &= A_1 + A_2a + A_3a^2 \\
A_1 &= Q_1 + x_eQ_2 + y_eQ_3 + x_ey_eQ_4 \\
A_2 &= x_vQ_2 + y_vQ_3 + (x_vy_e + y_vx_e)Q_4 \\
A_3 &= x_vy_vQ_4
\end{aligned} \tag{4}$$

If  $A_3$  is nonzero, the minimum (or maximum) value  $w_c$  of  $q(x, y)$  along  $L$  is found by computing the zero of the derivative of  $w$  and is given by

$$w_c = w(a^*), \quad a^* = \frac{-A_2}{2A_3}, \quad (5)$$

and if  $w_c$  falls within the neighborhood,  $d_N$  is the minimum of  $\{w(a^i), w(a^j), w_c\}$ , where  $m(a^i)$  and  $m(a^j)$  are the two points on  $L$  which fall on the boundary of the neighborhood. If  $w_c$  does not fall within the neighborhood, or if  $A_3$  equals zero, then  $d_N$  is the minimum of  $\{w(a^i), w(a^j)\}$ . Figure 7 shows a 2D example of the different types of minima. Now, let  $\{d_N\}$  be the set of minimum distances associated with the set of all four-pixel neighborhoods through which  $L$  passes. Then, the minimum distance  $d$  along  $L$  is determined as the minimum of the set  $\{d_N\}$ . This process is extendable to the 3D case, where  $d$  is determined by minimizing the trilinear interpolant function over each 8 voxel neighborhood through which the line passes.

Determining whether the drill burr along line  $L$  will hit surface  $S$  can now easily be defined by the following criterion. For any given path  $L$ , if  $d$  is greater than the radius  $r$  of the drill burr, then a burr following line  $L$  will miss surface  $S$ . If  $d$  is less than  $r$ , then a drill burr following  $L$  will hit  $S$ .

### Detecting effectiveness

There are two properties that a trajectory must satisfy to be effective and thus allow easy insertion of the electrode array into the scala tympani: (1) the well created by a drill burr following that trajectory must create an entrance into the scala tympani of diameter

greater than the that of the electrode array so that insertion is possible, and (2) since the array has a certain degree of rigidity and damage to the soft tissue of the scala tympani is undesirable, the well should be oriented at a similar angle to the axis of the scala tympani such that the entire process of insertion of the array into the scala tympani via the well is smooth. Both of these properties can be captured through a fairly simple criterion: the properties are said to be satisfied if a cylinder of radius  $\rho = 0.26$  mm (the radius of the tip of the electrode array) and length  $\gamma$  centered around the drilling trajectory can fit within the segmented scala tympani surface, where  $\gamma$  was chosen by an experienced physician to be 2.0 mm (see Figure 8).

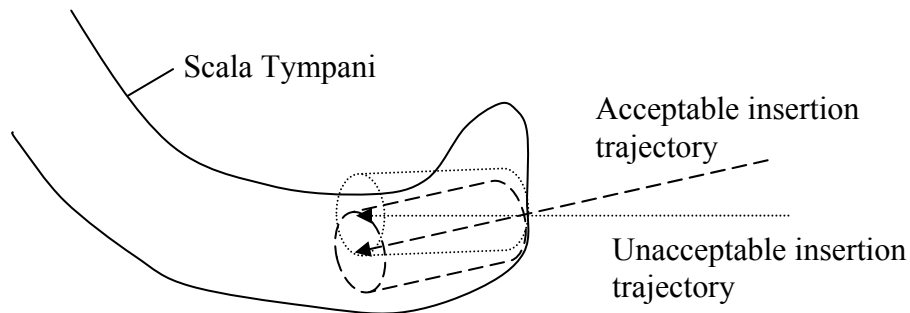


**Figure 8.** Examples of trajectories which are acceptable and unacceptable for insertion. As illustrated in the figure, detecting whether the cylinder surrounding the trajectory exits the structure can be used to decide whether electrode insertion will be feasible and smooth.

To measure whether this criterion is met, a cylinder along the trajectory is approximated by a discrete set of points. The points were chosen to be distributed around the trajectory at every  $\pi/4$  radians and along the trajectory every 0.3 mm. A point along the cylinder lies



outside (inside) the scala tympani if the distance map representing the scala tympani is greater than or equal to 0 (less than 0) at that point. With this information it is possible to determine the longest length along the drilling trajectory for which this cylinder lies entirely within the structure. If that length is larger than  $\gamma$ , then the trajectory is said to be acceptable with respect to the target structure.

### Probability of success calculations

With a method of determining whether any given drill trajectory contacts a sensitive structure and whether it appropriately reaches the target structure, a safety probability model can be constructed using a Monte Carlo approach. In this application, the target point is expected to experience isotropic, normally distributed error, while error at the skull entry point is negligible because it is so close to the center of the fiducial system. Therefore, using a normally distributed pseudorandom number generator, a vector  $q$  of dimensions  $3 \times 1$  is created such that each component of  $q$  is drawn from the zero-mean normal distribution with standard deviation  $\sigma$ . Given that  $\sigma_{\text{RMS}}$  is the expected RMS error at the target point,  $\sigma$  is computed using the equation

$$\sigma = \frac{\sigma_{\text{RMS}}}{\sqrt{3}}. \quad (6)$$

$q$  is then used to displace the trajectory at the site of the selected target position to  $p_t' = p_t + q$ . To determine whether the displaced path would damage a particular structure,  $d$  is

computed for the displaced path using Eqns. (1) and (2), and a ‘hit’ or ‘miss’ for the structure is determined. If a ‘hit’ or ‘miss’ is recorded iteratively for each iteration using a new random displacement  $q$ , a large set of hits or misses can be collected. Given a large enough number of iterations, the probability that the original drilling trajectory can successfully avoid damage to a particular surface,  $P_s$ , can be approximated by

$$P_s \cong \frac{n^{\text{misses}}}{n^{\text{misses}} + n^{\text{hits}}}, \quad (7)$$

where  $n^{\text{misses}}$  denotes the number of misses over all iterations and  $n^{\text{hits}}$  is defined similarly. Through experimentation, it was found that 10,000 iterations was sufficient. Beyond this number the probabilities remained the same to three significant digits.  $P_s$  is the quantified measure of safety that a drill burr following path  $L$  will not damage structure  $S$ .

The same process is applied to estimate  $P_T$ , the probability that any given drill path will be effective with respect to its target surface.  $P_T$  can be approximated by

$$P_T \cong \frac{n^{\text{effective}}}{n^{\text{not effective}} + n^{\text{effective}}}, \quad (8)$$

where  $n^{\text{effective}}$  is the number of displaced trajectories which are effective and  $n^{\text{not effective}}$  is defined similarly.

## Drilling trajectory optimization

The drilling trajectory is defined as the line that includes the skull entry point  $p_e$  and scala tympani target point  $p_t$ . Different possible trajectories are generated by varying  $p_e$  and  $p_t$ . The undesirability, or cost, of any given trajectory is determined from the probability values generated as described above using the simple function

$$c = -\left(b_1 \log(P_{S_1}) + b_2 \log(P_{S_2}) + b_3 \log(P_{S_3}) + b_4 \log(P_{S_4}) + b_5 \log(P_T)\right), \quad (9)$$

where  $S_1$ ,  $S_2$ ,  $S_3$ , and  $S_4$  denote the facial nerve, external ear canal, ossicles and chorda surfaces, and  $b_1$ ,  $b_2$ ,  $b_3$ ,  $b_4$ , and  $b_5$  denote constant coefficients. Note that the formula in Eq. (9) does not represent a probability, but is simply a way to combine five probabilities into one scalar value that can be optimized by some searching method. The logarithm functions weigh the effect of lower probability values greater relative to higher ones, while the coefficients are used to weight each logarithm term with a relative importance. Values for coefficients  $b_{1-5}$  may be derived using any appropriate method. In this application, it makes sense to derive these coefficients based on goals for safety and effectiveness established by an experienced surgeon. Goals for safety were decided to be probabilities of 0.999, 0.950, 0.800, and 0.800 for avoiding damage to the facial nerve, external ear canal wall, ossicles, and chorda; and 0.800 for effectively targeting the scala tympani. These are the probability levels that are necessary to guarantee that the percutaneous approach is at least as safe and effective as traditional methods. The relative weighting of the goals can be understood by recognizing that damage to the facial nerve is the most catastrophic, followed by violation of the external auditory canal, then

damage to the ossicles and chorda. Because it is desirable for implant insertion to be at least as effective as traditional methods, the goal for effectiveness is chosen just above the average effective implantation rate ( $\sim 73\%$ ). A planned trajectory is deemed acceptable if the trajectory's probability levels meet this set of goals. To account for these goals in the cost function, the coefficients  $b_{1-5}$  are chosen such that each of the probability terms contributes approximately equally to the cost function in the vicinity of the goals. Equality is achieved by choosing values of the coefficients such that

$$b_n = \frac{b_m \log((G_m))}{\log(G_n)}, \quad (10)$$

where  $n$  denotes the  $n$ th term in the cost function,  $m$  denotes the  $m$ th term, and  $G_n$  and  $G_m$  are the respective goals. Since only relative values affect the optimization, coefficient  $b_5$  was arbitrarily set to 1, and coefficients  $b_{1-4}$  were calculated using Eq. (10) to be 223.03, 4.35, 1.0, and 1.0.

Any appropriate searching method can be employed to minimize Eq. (9). Here, Powell's direction-set method with Brent's line-minimization algorithm is used [11]. A pair of orthogonal search directions  $\bar{v}_1$  and  $\bar{v}_2$  are chosen orthogonal to the specified initial drilling trajectory. In the search process, the components of  $p_t$  and  $p_e$  in these two directions are each varied independently, constituting 4 degrees of freedom. Constraining the search space to these four dimensions, rather than varying both points in 3D space, simplifies the optimization process while still allowing any plausible trajectory to be represented.

## CHAPTER V

### EXPERIMENTAL RESULTS

All programs were written in C++. The initial trajectory was specified using the methods presented in [9]. All sensitive structures were localized automatically using an atlas-based strategy as presented in [12],[13] combined with other techniques [14]. The drill burr used for the proposed surgery has a radius of 0.5mm. A complete optimization requires 1-2 minutes on a 2.4 GHz Intel Xeon Processor machine.

Experiments were conducted using patient CT scans of four left and nine right normal ears. Experiments followed Institutional Review Board approved protocols. For each ear in the dataset, drilling trajectories were generated with the fully automatic approach at both target positioning error levels of 0.44 and a more conservative level of 0.52 (~120% of 0.44) mm RMS, and a third trajectory was chosen manually by an experienced physician on the basis of visual inspection of the CT images. The results are shown in Table 1 for each of 13 ears from CT volumes of 10 patients (one ear per column).

**Table 1.** Drilling trajectory safety results across test subjects. Shown are probabilities of safety that the automatic initialization, automatically optimized, and manually chosen trajectories do not damage the sensitive structures and probabilities of effectiveness that they reach the target point in a manner conducive to smooth electrode array insertion. Numbers shown in bold are below the goals for safety for the manual and optimized trajectories.

Volume			1		2		3	4	5	6	7	8	9	10		Goals	
Ear			L	R	L	R	L	R	R	R	R	R	R	L	R		
Error Level	Trajectory	Probabilities of Safety or Effectiveness														Goals	
		Facial Nerve	0.44 mm	Initial	1.000	1.000	1.000	1.000	1.000	1.000	1.000	1.000	1.000	1.000	1.000		1.000
Optimized	1.000			1.000	1.000	1.000	1.000	1.000	1.000	1.000	1.000	1.000	1.000	1.000	<b>0.991</b>	<b>0.994</b>	
Manual	1.000			1.000	<b>0.993</b>	<b>0.997</b>	1.000	1.000	1.000	1.000	1.000	1.000	1.000	<b>0.993</b>	<b>0.636</b>	<b>0.854</b>	
0.52 mm	Initial		1.000	1.000	1.000	1.000	1.000	1.000	0.997	1.000	1.000	1.000	1.000	1.000	0.960	0.714	
	Optimized		1.000	1.000	1.000	1.000	1.000	1.000	1.000	1.000	1.000	1.000	1.000	0.999	<b>0.996</b>	<b>0.996</b>	
	Manual		1.000	0.999	<b>0.983</b>	<b>0.990</b>	<b>0.997</b>	1.000	1.000	<b>0.998</b>	1.000	1.000	1.000	<b>0.977</b>	<b>0.622</b>	<b>0.810</b>	
External Auditory Canal	0.44 mm	Initial	1.000	1.000	1.000	1.000	1.000	1.000	1.000	1.000	1.000	1.000	1.000	1.000	1.000	0.950	
		Optimized	1.000	1.000	1.000	1.000	1.000	1.000	1.000	1.000	1.000	1.000	1.000	1.000	1.000		
		Manual	1.000	1.000	1.000	1.000	1.000	1.000	1.000	1.000	1.000	1.000	1.000	1.000	1.000		
	0.52 mm	Initial	1.000	1.000	1.000	1.000	1.000	1.000	1.000	1.000	1.000	1.000	1.000	0.999	1.000		1.000
		Optimized	1.000	1.000	1.000	1.000	1.000	1.000	1.000	1.000	1.000	1.000	1.000	1.000	0.998		0.999
		Manual	1.000	1.000	1.000	1.000	1.000	1.000	1.000	1.000	1.000	1.000	1.000	1.000	1.000		1.000
Ossicles	0.44 mm	Initial	1.000	1.000	1.000	1.000	1.000	0.999	1.000	1.000	1.000	1.000	1.000	1.000	0.997	0.800	
		Optimized	0.999	1.000	0.998	0.999	0.995	0.999	1.000	1.000	1.000	1.000	1.000	1.000	1.000		
		Manual	1.000	1.000	1.000	1.000	1.000	0.980	0.946	0.912	1.000	1.000	0.902	0.970	0.999		
	0.52 mm	Initial	1.000	0.999	0.998	0.999	0.998	0.994	0.999	1.000	1.000	1.000	1.000	1.000	0.998		0.990
		Optimized	0.999	0.992	1.000	0.994	0.982	0.983	0.999	1.000	0.999	1.000	0.999	1.000	1.000		
		Manual	1.000	0.999	1.000	1.000	1.000	0.955	0.987	0.862	0.996	1.000	0.856	0.937	0.998		
Chorda	0.44 mm	Initial	0.407	1.000	0.685	0.954	0.949	0.799	1.000	0.987	1.000	0.998	0.074	0.346	0.964	0.800	
		Optimized	1.000	1.000	1.000	0.997	1.000	1.000	0.983	0.999	1.000	1.000	0.960	<b>0.256</b>	<b>0.477</b>		
		Manual	0.946	1.000	1.000	1.000	1.000	1.000	0.985	1.000	1.000	1.000	0.811	0.948	0.940		
	0.52 mm	Initial	0.411	1.000	0.650	0.913	0.907	0.754	0.998	0.967	0.998	0.991	0.111	0.361	0.939		
		Optimized	0.999	1.000	0.999	0.982	0.994	0.998	0.899	0.992	1.000	0.997	0.867	<b>0.104</b>	<b>0.323</b>		
		Manual	0.906	1.000	0.999	1.000	1.000	1.000	0.982	0.998	1.000	0.997	<b>0.777</b>	0.916	0.909		
Smooth Insertion	0.44 mm	Initial	0.875	0.788	0.858	0.820	0.887	0.813	0.791	0.873	0.882	0.717	0.868	0.815	0.728	0.800	
		Optimized	0.975	0.945	0.954	0.926	0.983	0.978	0.928	0.956	0.982	0.949	0.917	<b>0.495</b>	0.836		
		Manual	0.927	0.809	0.924	0.952	0.966	<b>0.706</b>	0.937	0.872	0.971	<b>0.007</b>	<b>0.477</b>	<b>0.061</b>	<b>0.010</b>		
	0.52 mm	Initial	0.799	0.710	0.777	0.723	0.814	0.745	0.711	0.789	0.830	0.644	0.805	0.728	0.664		
		Optimized	0.926	0.847	0.932	0.828	0.925	0.942	0.851	0.864	0.936	0.898	<b>0.748</b>	<b>0.297</b>	<b>0.484</b>		
		Manual	0.862	<b>0.748</b>	0.877	0.905	0.915	<b>0.619</b>	0.863	0.800	0.926	<b>0.013</b>	<b>0.460</b>	<b>0.075</b>	<b>0.021</b>		
			Cost Function Value														
	0.44 mm	Initial	0.448	0.103	0.231	0.154	0.075	0.188	0.102	0.065	0.055	0.145	1.192	2.480	26.502		
		Optimized	0.011	0.025	0.021	0.064	0.010	0.010	0.040	0.020	0.008	0.023	0.055	1.761	0.974		
		Manual	0.057	0.092	0.705	0.308	0.015	0.160	0.078	0.099	0.013	2.155	1.128	44.491	17.107		
	0.52 mm	Initial	0.484	0.149	0.298	0.181	0.133	0.253	0.437	0.117	0.082	0.195	1.051	4.531	32.396		
		Optimized	0.034	0.076	0.031	0.092	0.044	0.034	0.117	0.067	0.029	0.048	0.284	1.897	1.191		
		Manual	0.107	0.222	1.696	1.004	0.326	0.228	0.125	0.354	0.035	1.887	2.738	46.557	21.853		

This table gives the probabilities of safety for each of the four anatomic structures (Facial Nerve through Chorda) and the probabilities of effectiveness (Smooth Insertion). For each case, probabilities are given for six trajectories. These trajectories are the initial trajectory, the optimized trajectory, and the manually selected trajectory as determined

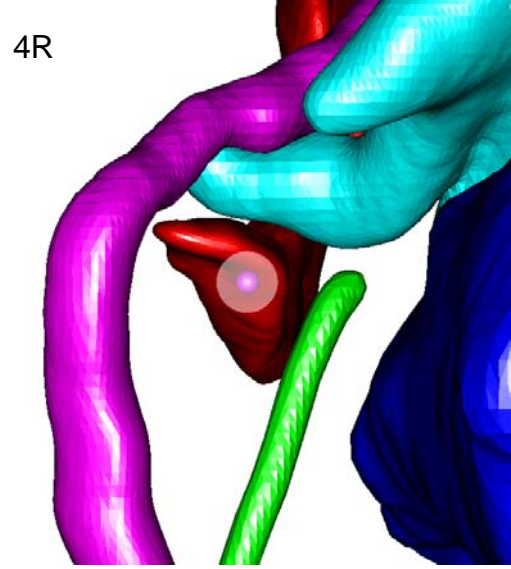
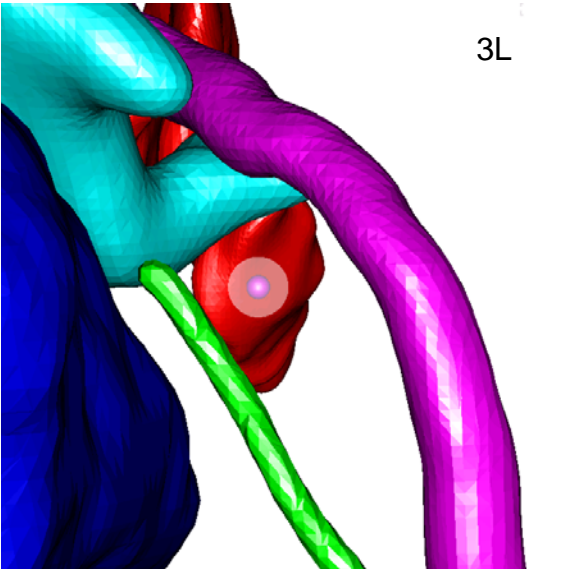
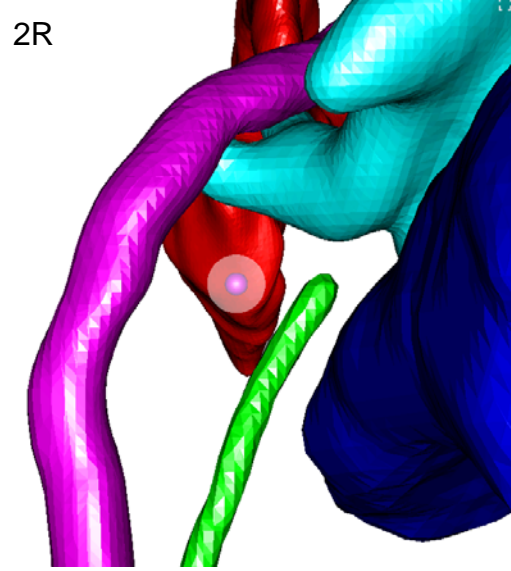
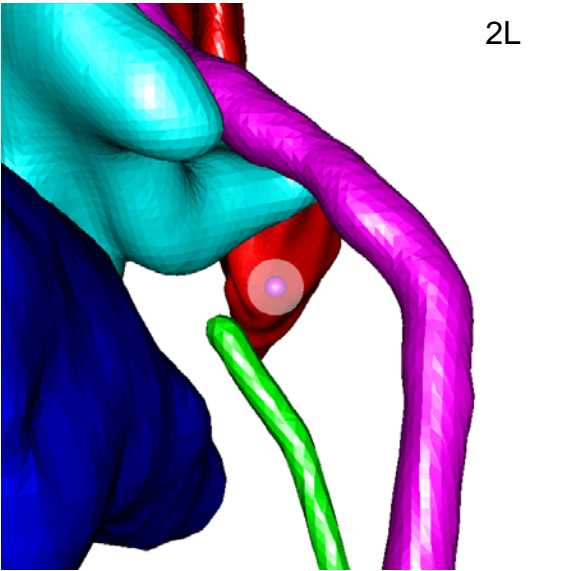
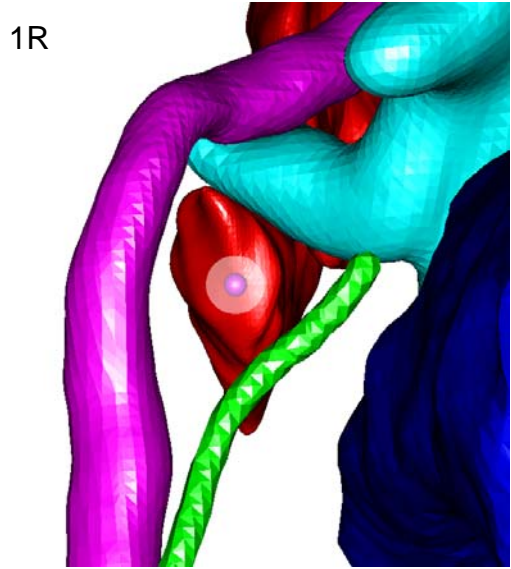
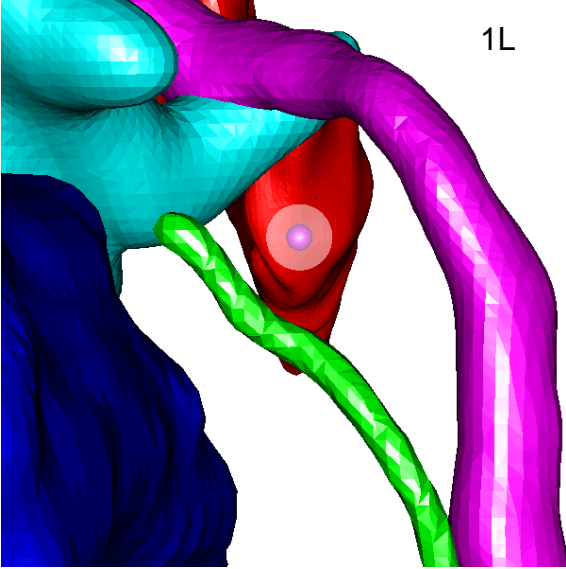
for each of the two error levels of target positioning (0.44 mm and 0.52 mm). In addition, at the bottom of the table, the value of the cost function corresponding to each trajectory is given. As mentioned above, the probabilities of success for the planned trajectories with respect to the structures were calculated via 10,000 trials of randomly displaced paths. Several probabilities of 1.000 are listed in the table. While in reality this is clearly impossible, those trajectories endured all trials without hitting the relevant structure. Given the calculation methodology, those probabilities of success are approximately 1.000.

Very positive results can be seen for most of the experimental trials. The numbers shown in bold indicate probability levels that fail to meet the goals. At a level of 0.44 mm RMS in drill positioning error, the trajectory optimization algorithm meets the goals for safety for all but the two ears of volume 10. It is especially of note that the optimization algorithm substantially decreases the safety of the chorda with respect to the initial position. This occurred, because both the left and right facial recess regions for this individual have a width of approximately 1.0~1.5 mm. Thus, fitting a 1.0 mm diameter trajectory between the facial nerve and chorda that meets all goals for safety given the estimation of error is not possible. The optimization algorithm heavily favors safety of the facial nerve, so as the facial nerve is made safe, the chorda is sacrificed. With these relatively low safety estimations, percutaneous implantation might not be recommended for this particular individual. Manually chosen trajectories at this error level fail to meet the safety goals on seven ears. In the ears of volume 10, the manually chosen trajectories significantly jeopardize the integrity of the facial nerve. Similar characteristics are seen at

the higher error level, where the goals are not met in 3 of 13 cases for the automatic trajectory and 10 of 13 for the manual trajectories. Thus, for the range of errors considered in this research, the automatic method found approximately twice as many safe and effective trajectories as the manual method.

It can be seen that even for initial positions whose probabilities are well below those of the manually selected trajectories, the automatic method consistently achieves its goals. In all cases, the optimization algorithm converges to a solution exhibiting a lower cost than manually chosen trajectories. These results suggest that the employed optimization method is indeed effective and robust in this application. 3-D renderings of the automatically generated trajectories are shown in Figure 9. Although precise safety estimations are difficult to determine with the human eye, all generated trajectories appear visually to be reasonable and safe.

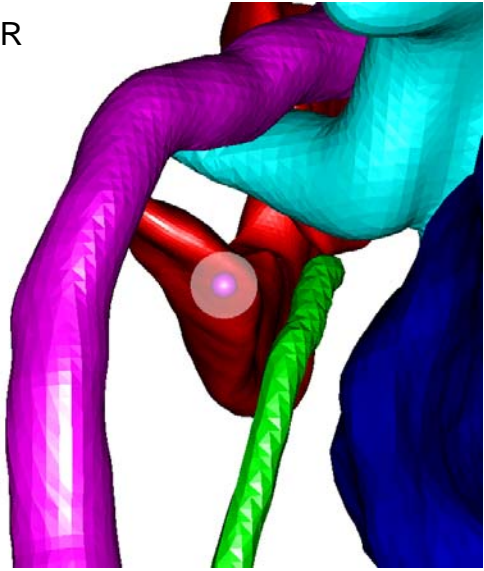




5R



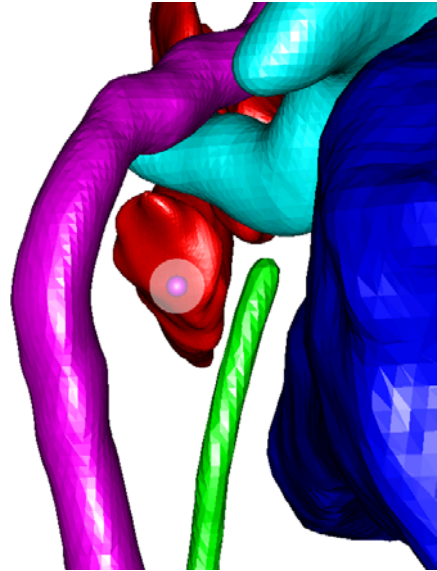
6R



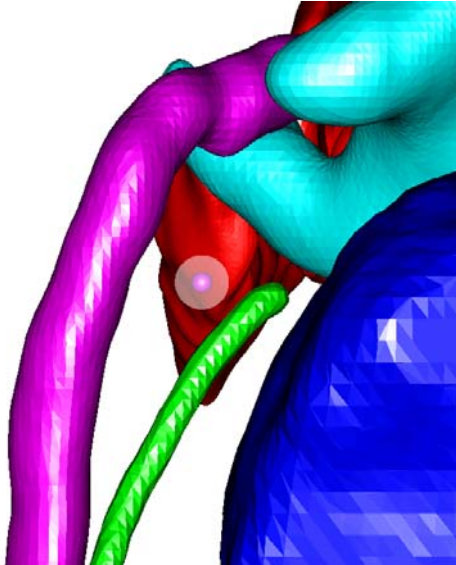
7R



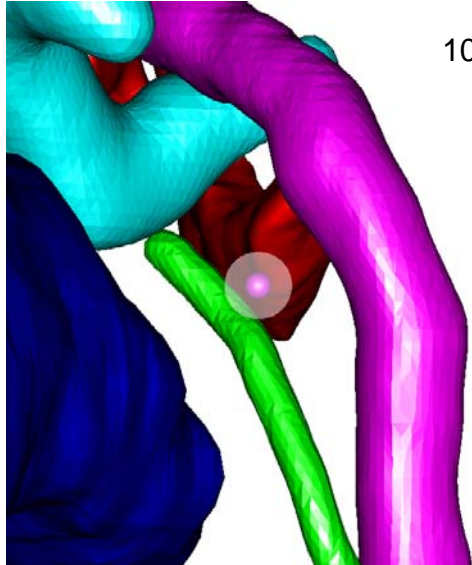
8R



9R



10L



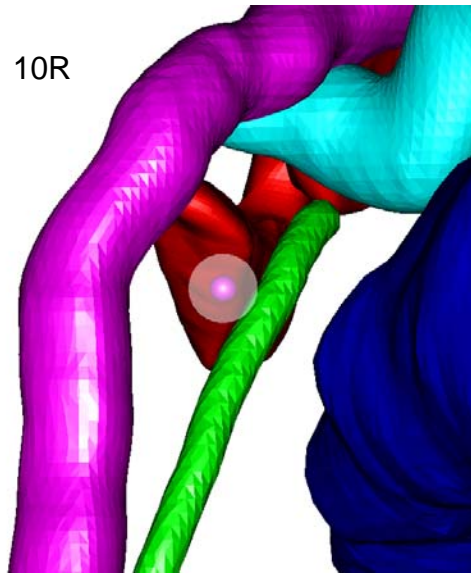


**Figure 9.** View along optimized trajectories (1.0 mm diameter circle). Anatomy is analogous to Figure 5. The figures are labeled according to the corresponding column in Table 1.

## CHAPTER VI

### DISCUSSIONS AND CONCLUSIONS

This thesis has presented a method to compute the safety of a given drilling trajectory, as well as a method for automatically finding a safe drilling trajectory for cochlear implant surgery. These results suggest that percutaneous cochlear access may be a viable alternative to traditional surgical methods for placing cochlear implants. With the current estimation of drill positioning error at the entrance to the cochlea, manual determination of drilling trajectories is prone to high variability in safety. Using the method presented in this thesis, however, safe trajectories can be automatically determined quickly and consistently. Unlike manual path selection, the automatic method accounts for error in the drill platform system, estimates the relative safety of any path in statistical terms, and indicates whether percutaneous access may be preferable to traditional methods for a specific patient. The results of this work suggest that percutaneous cochlear access may not be viable for a fraction of patients for a given level of error in drill positioning, and therefore this thesis has also demonstrated the benefits of error estimation to safely perform percutaneous cochlear implant surgery. While automatic trajectory determination appears to be feasible from this study, further clinical testing must be performed to better evaluate the difference in performance between manual and automatic trajectory decision.

## REFERENCES

- [1]. Gildenberg, Philip L and Tasker, Ronald R. *Textbook of stereotactic and functional neurosurgery*, McGraw-Hill Publishing (1998).
- [2]. P.E. Mohr, J.J. Feldman, J.L. Dunbar, A. McConky-Robbins, J.K. Niparko, R.K. Rittenhouse, and M.W. Skinner, "The societal costs of severe to profound hearing loss in the United States", *Int. J. Technol. Assess. Health Care* 16(4), 1120-1135, 2000.
- [3]. R.F. Labadie, P. Choudhury, E. Cetinkaya, R. Balachandran, D.S. Haynes, M. Fenlon, S. Jusczyk, J.M. Fitzpatrick, "Minimally-Invasive, Image-Guided, Facial-Recess Approach to the Middle Ear: Demonstration of the Concept of Percutaneous Cochlear Access In-Vitro", *Otol. Neurotol.* 26, 557-562, 2005.
- [4]. F.M. Warren, R.F. Labadie, R. Balachandran, J.M. Fitzpatrick, "Percutaneous Cochlear Access Using Bone-Mounted, Customized Drill Guides: Demonstration of Concept In-Vitro", Mtg. Am. Otologic Soc., Chicago, IL, May 2006.
- [5]. R.F. Labadie, J. Noble, B.M. Dawant, R. Balachandran, O. Majdani, J.M. Fitzpatrick, "Clinical Validation of Percutaneous Cochlear Implant Surgery: Initial Report", *Laryngoscope*. 2008;118: 1031-9.
- [6]. J.M. Fitzpatrick, P.E. Konrad, C. Nickele, E. Cetinkaya, C. Kao, "Accuracy of customized miniature stereotactic platforms", *Stereotactic and Functional Neurosurgery*, 83, 25-31, April 2005.
- [7]. R. Balachandran, J. Mitchell, B.M. Dawant, and J.M. Fitzpatrick, "Evaluation of targeting frames for deep-brain stimulation using virtual targets", *2007 4th IEEE International Symposium on Biomedical Imaging: Macro to Nano*, 1184-7, 2007.
- [8]. A. Aschendorff, J. Kromeier, T. Klenzner, and R. Laszig, "Quality Control After Insertion of the Nucleus Contour and Contour Advance Electrode in Adults", *Ear & Hearing*. 28, 75S-79S, April 2007.
- [9]. H. Al-Marzouqi, J. Noble, F. Warren, R.F. Labadie, J.M. Fitzpatrick, B.M. Dawant, "Planning a safe drilling path for cochlear implantation surgery using image registration techniques", *Progress in Biomedical Optics and Imaging - Proceedings of SPIE*, Volume 6509, pp. 650933, Feb. 2007.
- [10]. J. Sethian, *Level Set Methods and Fast Marching Methods*, 2nd ed. Cambridge, MA: Cambridge Univ. Press, 1999.
- [11]. W. H. Press, B. P. Flannery, S. A. Teukolsky, and W. T. Vetterling, *Numerical Recipes in C*, 2nd ed. Cambridge, U. K.: Cambridge Univ. Press, 1992, ch. 10, pp. 412-419.

- [12]. B.M. Dawant, S.L. Hartmann, J.P. Thirion, F. Maes, A. Vandermeulen, and P. Demaerel, “Automatic 3-D segmentation of internal structures of the head in MR images using a combination of similarity and free-form transformations. I. Methodology and validation on normal subjects”, *IEEE Trans. Med. Imag.* 1999;18-10:906-16.
- [13]. G.K. Rohde, A. Aldroubi, and B.M. Dawant, “The adaptive bases algorithm for intensity-based nonrigid image registration”, *IEEE Trans. Med. Imag.* 2003;22:1470-9.
- [14]. J.H. Noble, F.M. Warren, R.F. Labadie, and B.M. Dawant, “Automatic segmentation of the facial nerve and chorda tympani in CT images using spatially dependent feature values”, *Medical Physics.* 2008; 35(12):5375-84.